2016-09-15

Recent H-alpha results on pulsar B2224+65's bow-shock nebula, the "Guitar"

Recent H-alpha Results on Pulsar B2224+65's Bow-Shock Nebula, the "Guitar"

Timothy Dolch[1,2] †, Shami Chatterjee[2], Dan P. Clemens[3], James M. Cordes[2], Lauren R. Cashmen[3], Brian W. Taylor[3]

[1]Hillsdale College, Hillsdale, MI, USA
[2]Cornell University, Ithaca, NY, USA
[2]Boston University, Boston, MA, USA

† Corresponding Author
E-mail: tdolch@hillsdale.edu
Tel: +1 517-607-2449
ORCID: 0000-0001-8885-6388
Received June X, 2016, Revised ??, 2015 Accepted ??

Heading Title: T. Dolch et al. H-alpha Results on the Guitar Nebula
Article Type:

Keywords: ISM: Structure, Stars: Pulsars: Individual: Alphanumeric: PSR B2224+65, Shock Waves, Stars: Neutron

We used the 4m Discover Channel Telescope (DCT) at Lowell Observatory in 2004 to observe the Guitar Nebula, an Hα bow-shock nebula around the high-velocity radio pulsar B2224+65. Since the nebula's discovery in 1992, the structure of the bow-shock has undergone significant dynamical changes. We observe the limb structure, targeting the "body" and "neck" of the guitar. Comparing the DCT observations to 1995 observations with the Palomar 200-inch Hale telescope, we find changes in both spatial structure and surface brightness in the tip, head, and body of the nebula.

1. INTRODUCTION

Many pulsars throughout the Galaxy have high spindown energy outflows and/or high velocities. Under favorable conditions, they are accompanied by bow-shock pulsar wind nebulae with radio, optical, and/or X-ray structure. Recent bow-shock nebula search campaigns have targeted Fermi-LAT discovered pulsars (Romani et al. 2010, Brownsberger & Romani 2014) and have brought the list of currently known Hα bow-shock nebulae to nine. Bow-shock nebulae frequently occur around canonical (non-millisecond) pulsars, which are more likely to have high $\dot{E}$ values due to their young ages (where $\dot{E}$ is the spindown luminosity in erg/s), as well as high velocities compared to millisecond pulsars (MSPs). MSPs are often found in binary systems, thus having high escape velocities from the gravitational potential wells in which they originated.

The observability of extended bow-shock nebula structure depends on a variety of factors (Chatterjee & Cordes 2002; hereafter CC02). The surface brightness of a resolvable nebula, although a small fraction of the total energy output of the corresponding neutron star, will be proportional to $\dot{E}/D^2$, where D is the distance to the system in kpc. Limb-brightened structure is visible for higher values of the transverse velocity v_T in km/s. Higher values of the ambient interstellar medium (ISM) density n_H in cm^{-3} result in more energetic shocks; however, low ionization fractions are also required so that the radiative processes involved are primarily ram-pressure driven.

Understanding the ambient ISM near and around pulsars is important for studying the ambient density structure of the ISM in general. As some of the important factors influencing the timing accuracy of pulsars for their ability to detect gravitational waves (Cordes 2013, Stinebring 2013), variations in pulsar dispersion measure (DM), along with the presence of interstellar scattering and scintillation, all depend on the underlying structure of the ISM along the lines-of-sight (LOSs) to pulsars.

The Hα nebula around radio pulsar B2224+65, referred to as the "Guitar Nebula" (GN) is the most dynamic bow-shock system currently known. PSR B2224+65[1], an otherwise unremarkable canonical pulsar with period $P \sim 0.68$ s and an $\dot{E} \sim 1.2\times10^{33}$ erg/s, is amongst the highest velocity neutron stars known ($v_T \sim$

[1] http://www.atnf.csiro.au/people/pulsar/psrcat/

800 - 1700 km/s, the uncertainty arising from a distance 1 - 1.9 kpc). The GN was discovered as part of a Palomar Observatory survey of radio pulsars (Cordes et al. 1993), and the likely 90° inclination angle with respect to the LOS (CC02) means that any changing structures are maximally visible. The extremely high velocity was consistent with a natal velocity kick from an asymmetric supernova. A campaign of follow-up observations with the Palomar 200-inch Hale Telescope in conjunction with observations of the guitar head from the Hubble Space Telescope (HST) showed that the ambient ISM density decreased by a factor of 0.7, from 0.006 to 0.004 cm^{-3} for D = 1.9 kpc over 7 years (Chatterjee & Cordes 2004; hereafter CC04). These changes occurred over 1.3", or ~2500 AU. The expansion of the tip of the nebula was consistent with the radio proper motion measurement of 182±3 mas/yr (Harrison, Lyne, & Anderson 1993; hereafter HLA93). In addition to density gradients, the time sequence of observations revealed inhomogeneities that constrained the ISM's density fluctuation power spectrum. NRAO Very Large Array searches for nonthermal radio-synchrotron nebular structure resulted in non-detections. At X-ray energies, Chandra ACIS-S3 observations revealed an off-axis X-ray jet originating at the tip of the GN (Wong et al. 2003; Hui & Becker 2007). Hui et al. (2012), using XMM-Newton images, found X-ray flux near the pulsar, but no X-ray pulsations. No associated Fermi-LAT sources were found.

2. OBSERVATIONS

Motivated by the ~7yr dynamic timescale of the GN (CC04), we used Hα imaging at the 4.3m Discovery Channel Telescope (DCT) to observe the GN, 22 years after its original discovery. Using the Large Monolithic Imager[2] (LMI) with its 12.5' × 12.5' field of view, the DCT is extremely well-suited to image the largest lengthscales of the GN, enabling high-quality surface photometry down to 30 mag/arcsec^2 in the B and V bands.

Observations were taken at 24-Oct 2014 for 5hr, with about 86% of the time on the Hα ON filter (center wavelength 6564.9Å, bandwidth 30.1Å) and the remaining time spent on the Hα OFF filter (center wavelength 6459.1Å, bandwidth 114.6Å). Pixels were binned in 2×2 mode in order to reduce read noise, resulting in images with a 0.24" pixel scale. Apart from some very light cloud cover, the seeing remained high-quality, reaching toward 0.5" toward the end of the night. We compare these images to those from the 1995 Palomar observations with the 200-inch Hale Telescope and the 1994 HST images, both described in CC02.

The pointings were combined using IRAF/PyRAF tasks. We obtained an ON DCT image (Fig. 1) after appropriate scaling. Then, using the `geotran` task in IRAF, we aligned the 1995 Palomar image (Fig. 2) with the ON DCT image and found the difference image (Fig. 3) after appropriate time and bandwidth rescaling.

3. RESULTS

Fig. 3 shows the forward proper motion at the tip. The expansion around the edges of the bottom of the head is also apparent. Interestingly, the rounded body of the GN has also expanded, but the regions between have not, suggesting a higher density toward the middle of the nebula, confining the shocked medium. Figs. 4, 5, and 6 are the corresponding images to Figs. 1, 2, and 3, zoomed in on the head, except for Fig 4 which is the ON – OFF image with time and bandwidth scalings applied. The ON – OFF image removes one small background star from the head. The circled region in Fig. 4 shows possible sub-structure forming at the tip of the nebula. No corresponding stars are visible behind the present tip in the OFF image. The limb-brightened edges of the GN head appear piecewise and disconnected, suggesting a highly inhomogeneous region.

In CC02, symmetric and antisymmetric images were obtained by mirroring the HST image of the GN head along the symmetry axis of the GN and taking the sum and difference, respectively. (In the remaining analysis, we use the ON image rather than the ON – OFF image because of the frequent comparisons to the 1995 Palomar image, which used an ON image only.) We perform a similar analysis here and compare the results to those from the HST's Wide Field Planetary Camera 2 (WFPC2) in 1994. While the space-based

[2] `http://www2.lowell.edu/users/massey/LMIdoc.pdf`

WFPC2 data are obviously superior, especially given the detector's 0.0455" pixel scale, it is interesting to note how closely the DCT-LMI image quality approaches that of HST images from the WFPC2 era.

Finding the GN's true position angle (PA) is not trivial. Observations of PSR B2224+65 with the Lovell Telescope at Jodrell Bank Observatory in HLA93 report PA ~ 52.1°±0.9°, while bow-shock model fits in CC02 report PA ~ 48°±2°. One LMI pixel spans 1/225 of the GN's length. The minimum PA resolution available in these images is then ~0.25°. In order to find the effective PA for the DCT image of the GN head, we perform a grid search in PA from 47° to 50° in steps of 0.25°, and for each angle, create a rotated, repixelated image with the `rotate` task in IRAF and then search amongst 2 – 3 potential image columns for the axis of symmetry that minimizes the limb-brightened flux in the antisymmetric image. This process results in an effective PA of 49.25°, which we use for the remaining symmetric/anti-symmetric analysis. While PA ~ 49.25° effectively minimizes the antisymmetric flux from the GN head, it does not minimize the antisymmetric flux from the GN body. However, there are parameters in the grid search for angles on each side of 49.25° that reduce the GN body's antisymmetric flux much more significantly than does the 49.25°-rotated image. It is not surprising that the GN body fails to constrain the PA well, owing to its larger angular scale and more diffuse structure. A highly symmetric tip, however, is predicted by bow-shock simulations (Wilkin 1996).

The resulting rotated, symmetric, and anti-symmetric images are shown as Figs. 7, 8, and 9 respectively. In the rotated image, the asymmetries at the bottom of the GN head are more visually apparent than in the usual north-up image. The symmetric image (Fig. 8) highlights the suggestive sub-structure at the GN tip. The anti-symmetric image (Fig. 9), following CC02, is shown as follows. The original difference image is convolved with a 1-pixel Gaussian, and pixel absolute values <1σ are zeroed out, where σ is the image noise level, defined as the 10 sigma-clipped standard deviation of the original rotated image (Fig. 7).

In the circled region of Fig. 9, a number of interesting features are apparent. The parallel diagonal bands clearly show the asymmetric limb-brightened areas toward the bottom of the GN head. Such a radical spatial asymmetry was not present in the CC02 1994 HST images, in which the head asymmetry was primarily an asymmetry in the surface brightness of the limbs. Furthermore, the bottom of the head (toward the bottom of the marking circle) now appears to show a surface brightness asymmetry. As concluded in CC02, the surface brightness asymmetry is likely indicative of an ISM density gradient in a different direction than the neutron star's motion. More recently, however, this surface brightness asymmetry seems to have become present at the bottom of the head, and not only on the limb-brightened edges immediately behind the tip. Averaging over a number of corresponding pixels in the surface brightness asymmetry, we find that the ratio of antisymmetric surface brightness to the symmetric surface brightness is ~0.2. The spatially asymmetric structure requires a more complex model from which to draw further conclusions.

To estimate the forward motion at the tip, we take the central few columns of the difference image along the symmetry axis and sum them together in the direction perpendicular to the symmetry axis, resulting in a 1D array of values. When this array changes from negative to positive, it represents the beginning of the motion tracked since 1995. We therefore take the peak positive value as the 1995 tip position, and take the current tip position to be when the positive part of the array is equal to 1σ above the sky noise outside the GN tip. The difference in these pixel positions implies 170±20 mas/yr over the 19.33 years between images, which is within the uncertainties of the radio pulsar's motion from timing data. (The uncertainty assumes a 1 pixel error for the start and end of the expansion region in the difference image.)

Similarly, we estimate the expansion rate of the GN body by taking one cutout region of positive-negative parallel limb arcs indicating outward expansion. For this small region in which the limbs are barely curved, we sum along the long direction to obtain a 1D array with a peak and a trough. The width of the positive region that rises 3σ above the surrounding noise outside the GN altogether is about four pixels. These is equivalent to an expansion rate of 50±10 mas/year for the GN body.

4. CONCLUSIONS AND FURTHER WORK

Changes in the GN since 1995 as recently imaged by the DCT implies a 0.17"/yr proper motion at the tip, or about (0.007—0.011) *c*. The GN body expands at about 0.05"/yr. In the GN head, asymmetries in both limb-brightened spatial structure and in surface brightness appear to have occurred. Most intriguingly, additional substructure near the tip may have appeared. CC04 suggests that the head of the GN may be a second "guitar" undergoing formation. Should new structure at the tip prove significant, it may be the

beginnings of a third "guitar". However, we caution against over-interpretation, as the tip region is not resolvable from the ground, and requires further observations.

The GN's evolution between 1995 and 2014 supports the model of the GN as a series of expanding bubbles through an HI ISM with varying density. The density variations are likely sufficient to explain the asymmetries and varying structure densities in the limb-brightened regions. However, the structure of a bow-shock nebula is dependent on factors in addition to n_H, namely $\dot{E}$ and the ionization fraction of the surrounding medium. While Ockham's razor would seem to favor a varying n_H, it is intriguing to consider variations in $\dot{E}$, which could in principle correspond to timing glitches in PSR B2224+65, a number of which have been reported (Jansen & Stappers 2006, Yuan et al. 2010). Continued radio monitoring could therefore reveal Hα structure changes in correlation with glitch events. Also, a changing ionization fraction, or lack thereof, could be deduced from a DM monitoring campaign on the pulsar. Properties of the associated X-ray filament may also change on dynamic timescales, and would benefit from a periodic observing campaign with Chandra and/or Newton-XMM.

In a later paper, we will combine the large-scale analysis with a study of small scale structure down to about 0.1" that makes use of multi-epoch HST data. More detailed modeling of the GN that incorporates many epochs could shed light on the questions opened up by the recent DCT observation.

ACKNOWLEDGEMENTS

SJC, JMC, and TD were partially supported through the National Science Foundation (NSF) PIRE program award number 0968296. DPC and RLC acknowledge support from the NSF under AST09-07790 and AST14-12269. TD also thanks the Douglas R. Eisenstein research gift to Hillsdale College. These results made use of the Discovery Channel Telescope at Lowell Observatory, supported by Discovery Communications, Inc., Boston University, the University of Maryland, the University of Toledo and Northern Arizona University. PyRAF is a product of the Space Telescope Science Institute, which is operated by AURA for NASA. This research has made use of NASA's Astrophysics Data System.

REFERENCES

Brownsberger, S., & Romani, R. W. 2014, ApJ, 784, 154. http://dx.doi.org/10.1088/0004-637X/784/2/154

Chatterjee, S., & Cordes, J. M. 2002, ApJ, 575, 407. http://dx.doi.org/10.1086/341139

Chatterjee, S., & Cordes, J. M. 2004, ApJL, 600, L51. http://dx.doi.org/10.1086/381498

Cordes, J. M. 2013, Classical and Quantum Gravity, 30, 224002. http://dx.doi.org/10.1088/0264-9381/30/22/224002

Cordes, J. M., Romani, R. W., & Lundgren, S. C. 1993, Nature, 362, 133. http://dx.doi.org/10.1038/362133a0

Harrison, P. A., Lyne, A. G., & Anderson, B. 1993, MNRAS, 261, 113. http://dx.doi.org/10.1093/mnras/261.1.113

Hui, C. Y., Huang, R. H. H., Trepl, L., et al. 2012, ApJ, 747, 74. http://dx.doi.org/10.1088/0004-637X/747/1/74

Hui, C. Y., & Becker, W. 2007, A&A, 467, 1209. http://dx.doi.org/10.1051/0004-6361:20066562

Janssen, G. H., & Stappers, B. W. 2006, A&A, 457, 611. http://dx.doi.org/10.1051/0004-6361:20065267

Manchester, R. N., Hobbs, G.B., Teoh, A. & Hobbs, M. 2005, AJ, 129, 1993. http://dx.doi.org/10.1086/428488

Romani, R. W., Shaw, M. S., Camilo, F., Cotter, G., & Sivakoff, G. R. 2010, ApJ, 724, 908. http://dx.doi.org/10.1088/0004-637X/724/2/908

Stinebring, D. 2013, Classical and Quantum Gravity, 30, 224006. http://dx.doi.org/10.1088/0264-9381/30/22/224002

Wilkin, F. P. 1996, ApJL, 459, L31. http://dx.doi.org/10.1086/309939

Wong, D. S., Cordes, J. M., Chatterjee, S., et al. 2003, High Energy Processes and Phenomena in Astrophysics, 214, 135

Yuan, J. P., Wang, N., Manchester, R. N., & Liu, Z. Y. 2010, MNRAS, 404, 289. http://dx.doi.org/10.1111/j.1365-2966.2010.16272.x

Figure Captions

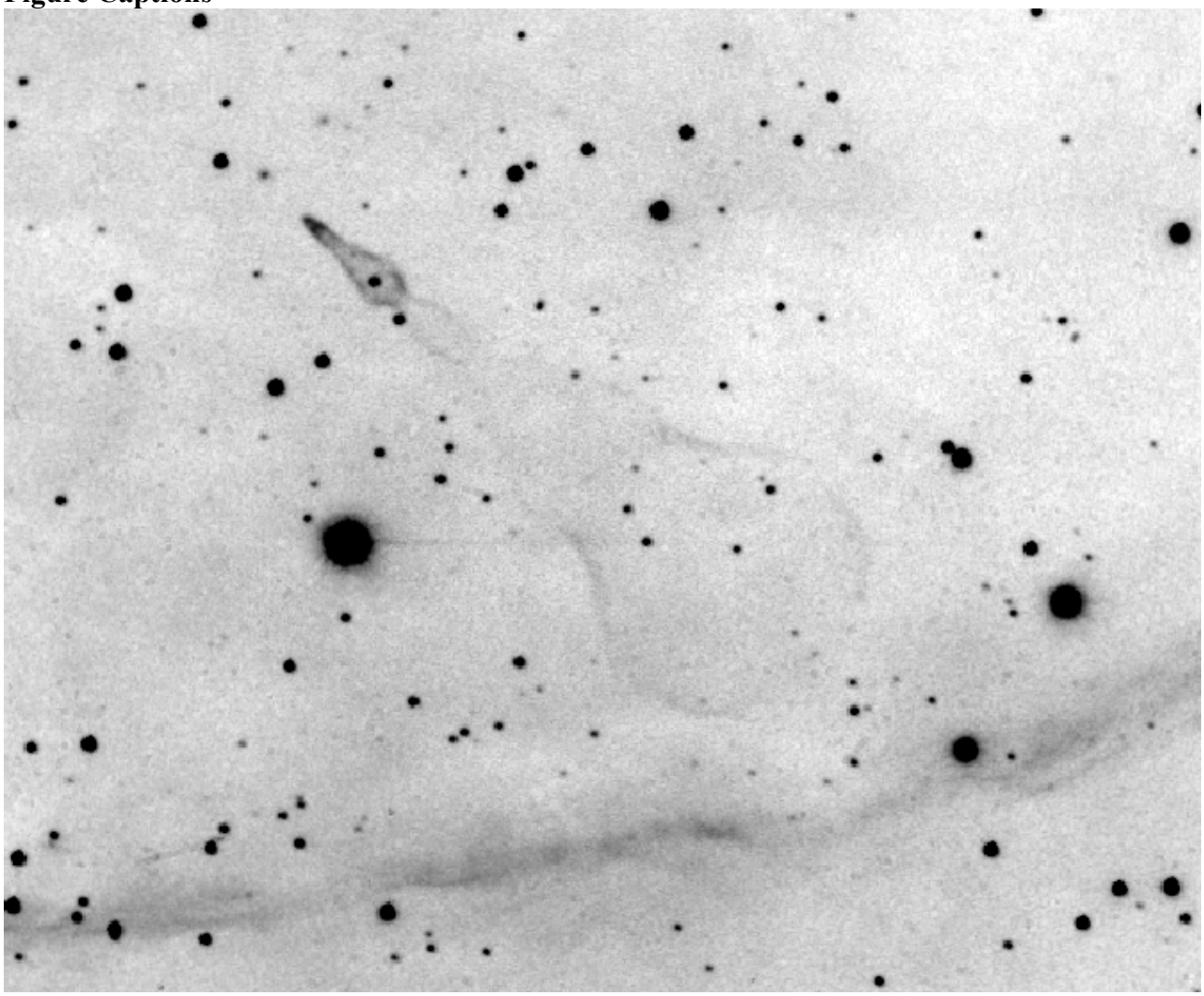

Fig. 1. Hα image of the Guitar Nebula (6564.9Å, bandwidth 30.1Å) taken with the 4.3m Discovery Channel Telescope at Lowell Observatory in late 2014. The sense of north is up, while east is left. The colormap is inverted. The large horizontal filament is in the Hα only and is not known to be related to the nebula.

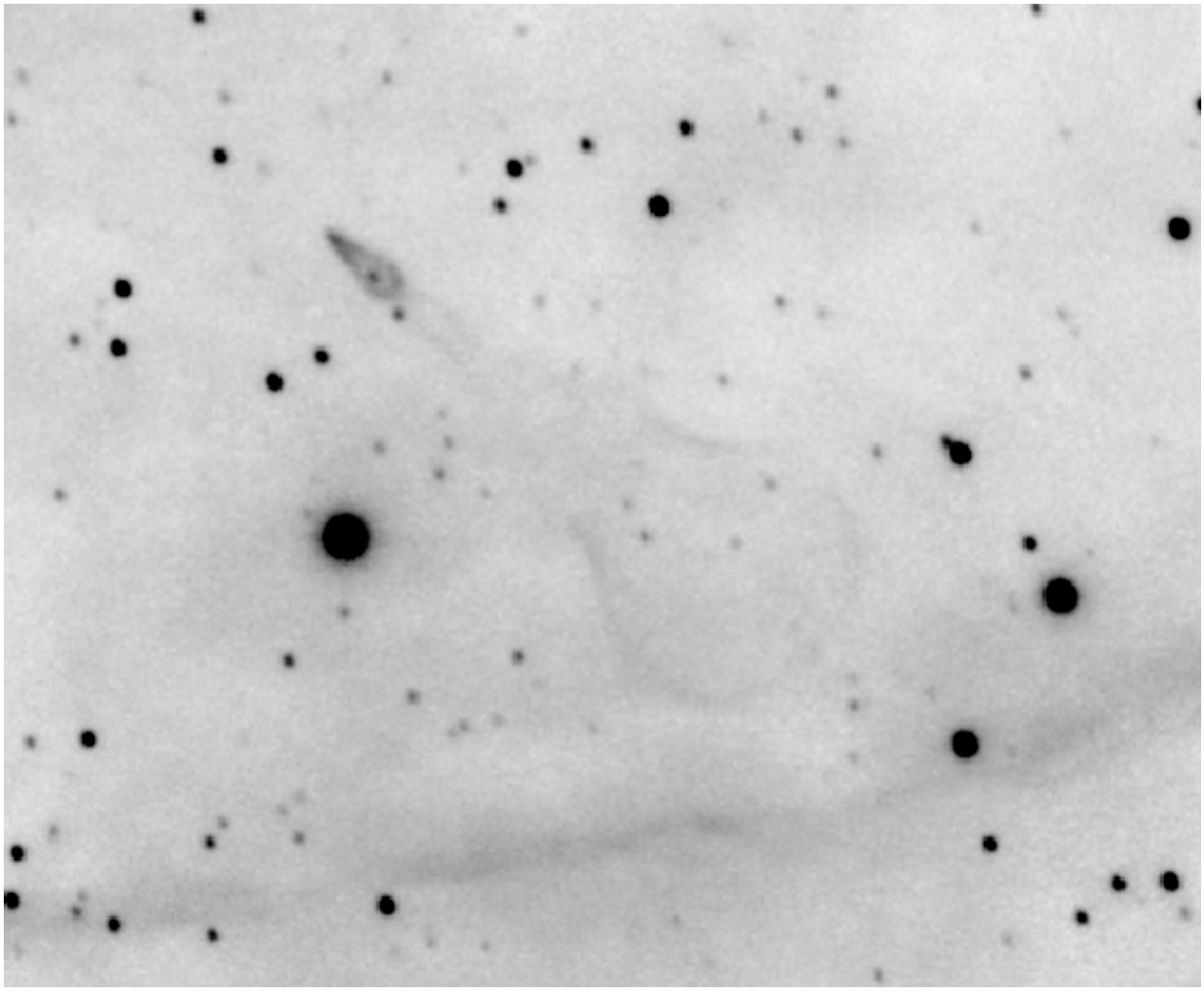

Fig. 2. Hα image of the Guitar Nebula (6564Å, bandwidth 20Å) from the 5m Hale Telescope at Palomar Observatory from 1995, described in CC02. The sense of north is up, while east is left. The colormap is inverted.

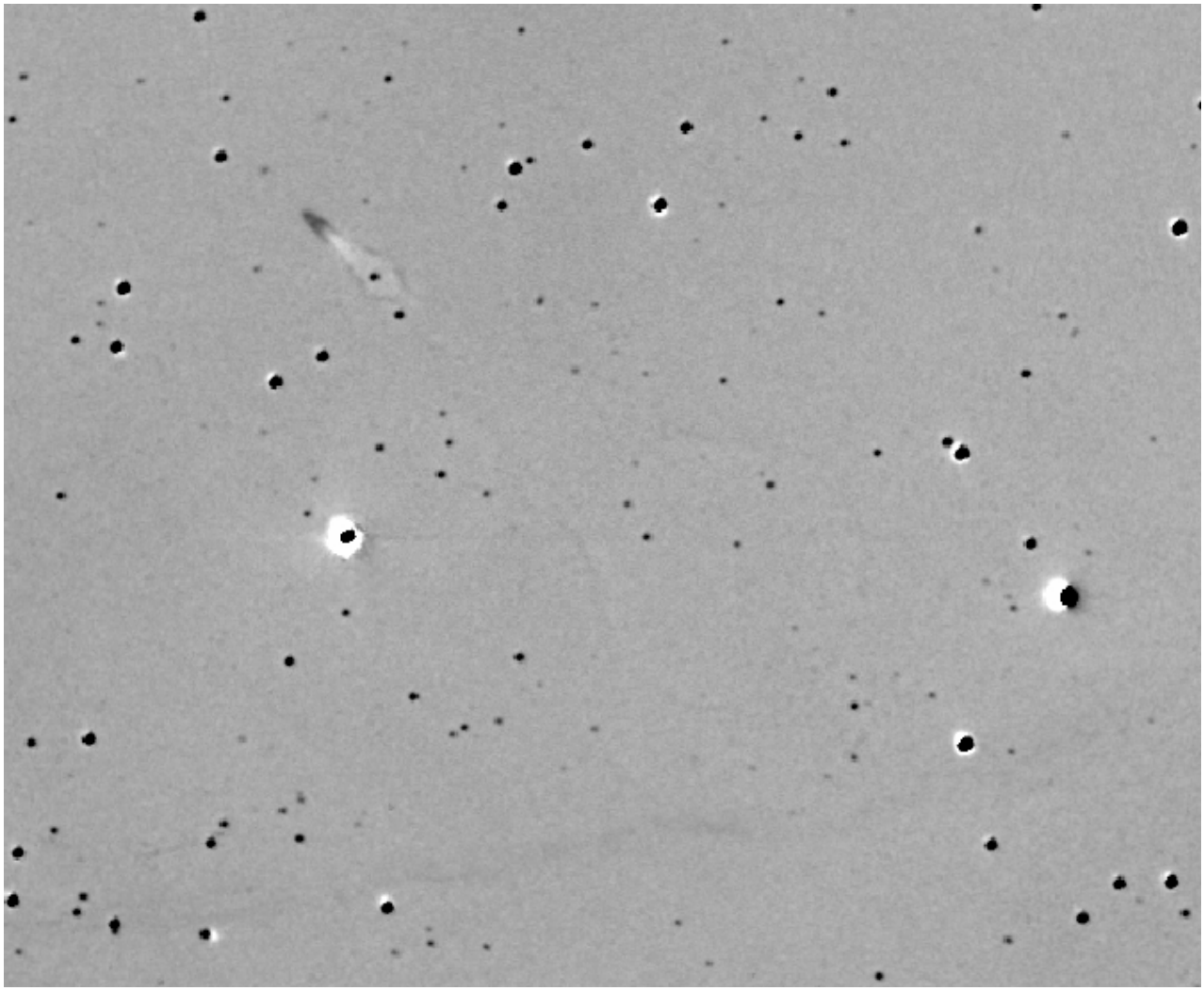

Fig. 3. Difference image between DCT and Palomar images showing changes in the Guitar Nebula over the 19.3yr between observations. The rounded body has expanded at 0.05"/yr, but the upper body and neck have undergone little expansion. The sense of north is up, while east is left. The colormap is inverted.

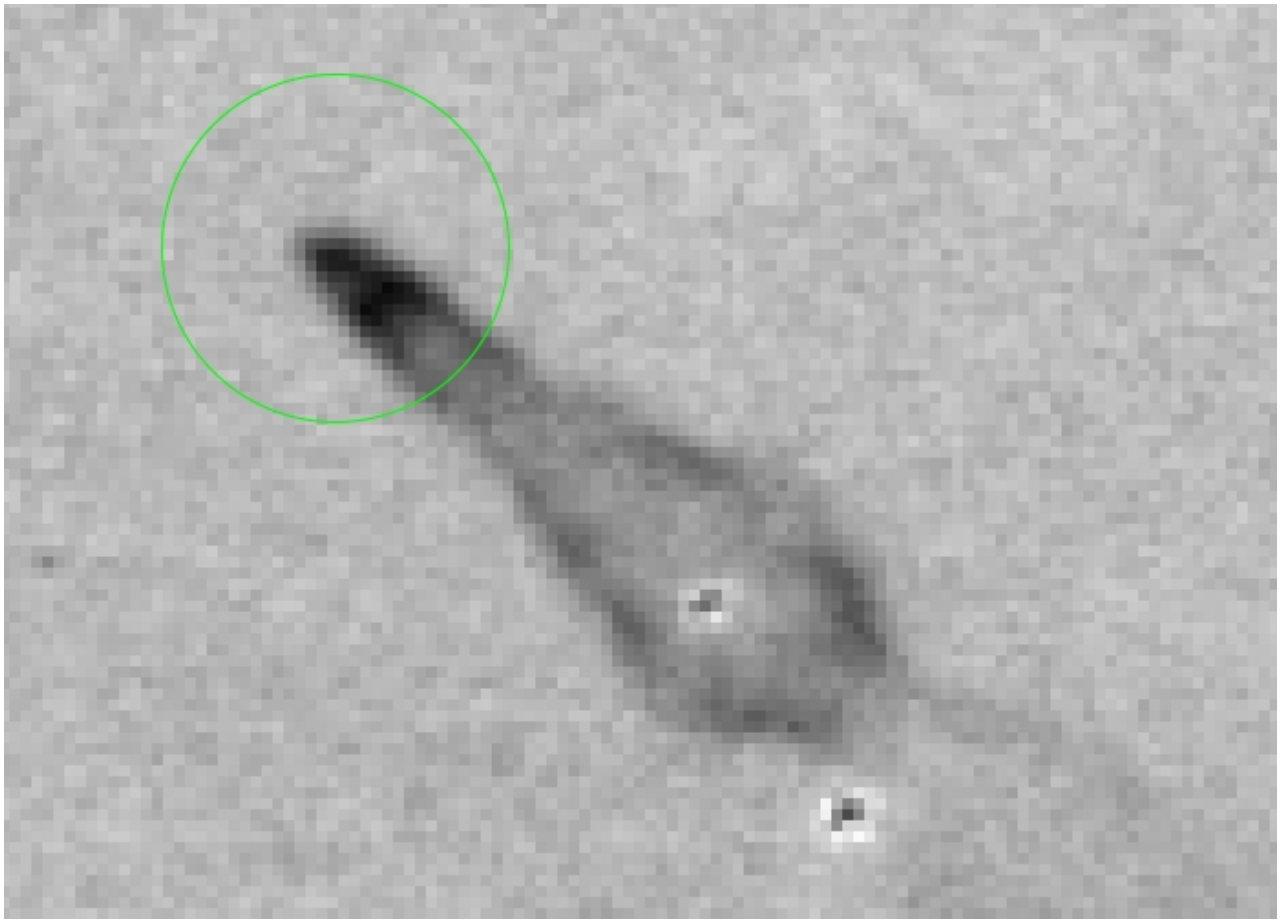

Fig. 4. Hα ON - OFF image of the Guitar Nebula (6564Å, bandwidth 20Å ON; 6459.1Å, bandwidth 114.6Å OFF) from the 5m Hale Telescope at Palomar Observatory from 1995, described in CC02. The sense of north is up, while east is left. The colormap is inverted. New substructure that may be forming in the tip is circled.

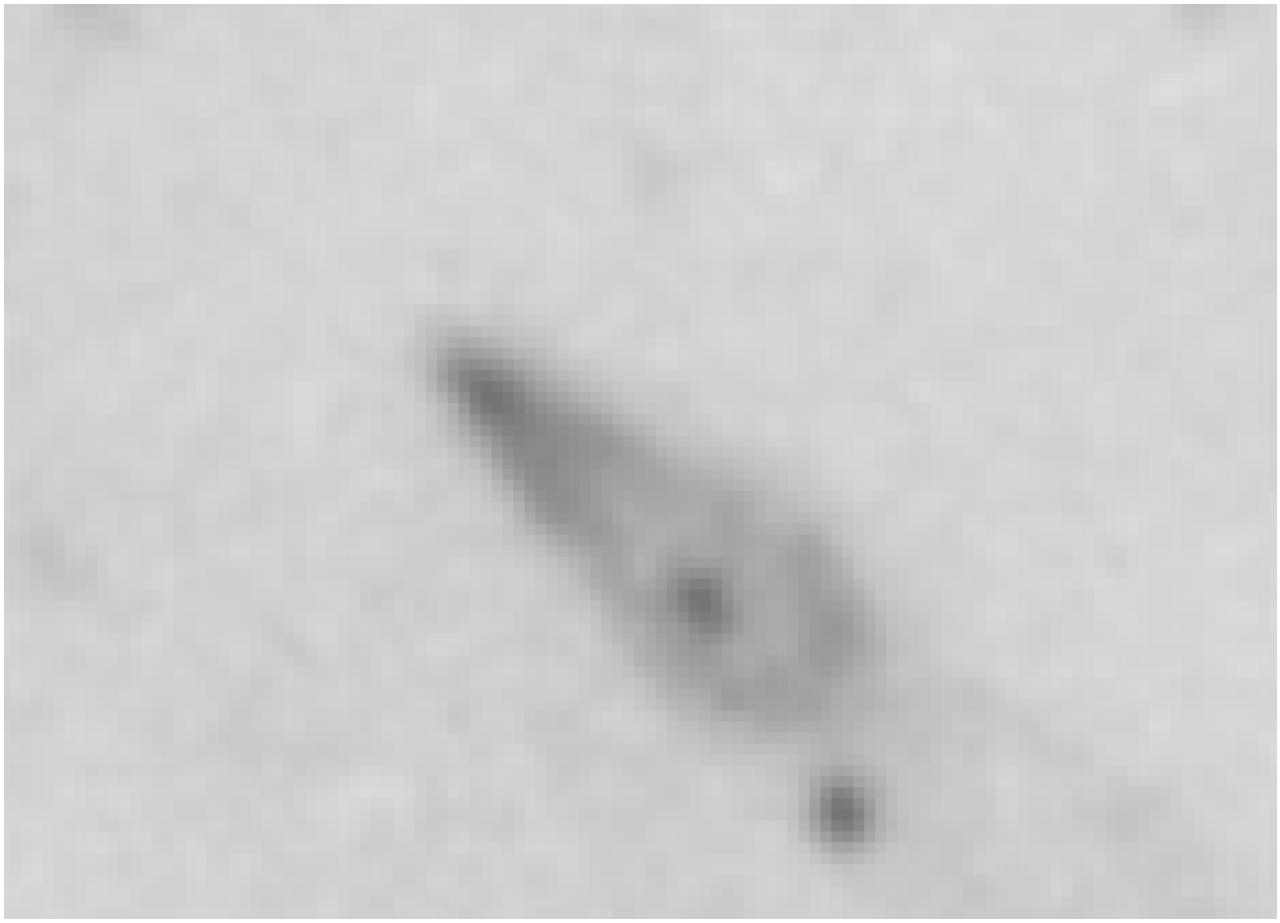

Fig. 5. Hα image of the Guitar Nebula head (6564Å, bandwidth 20Å) from the 5m Hale Telescope at Palomar Observatory from 1995, described in CC02. The sense of north is up, while east is left. The colormap is inverted. The cylindrical column between head and tip had not formed at the time the data were taken.

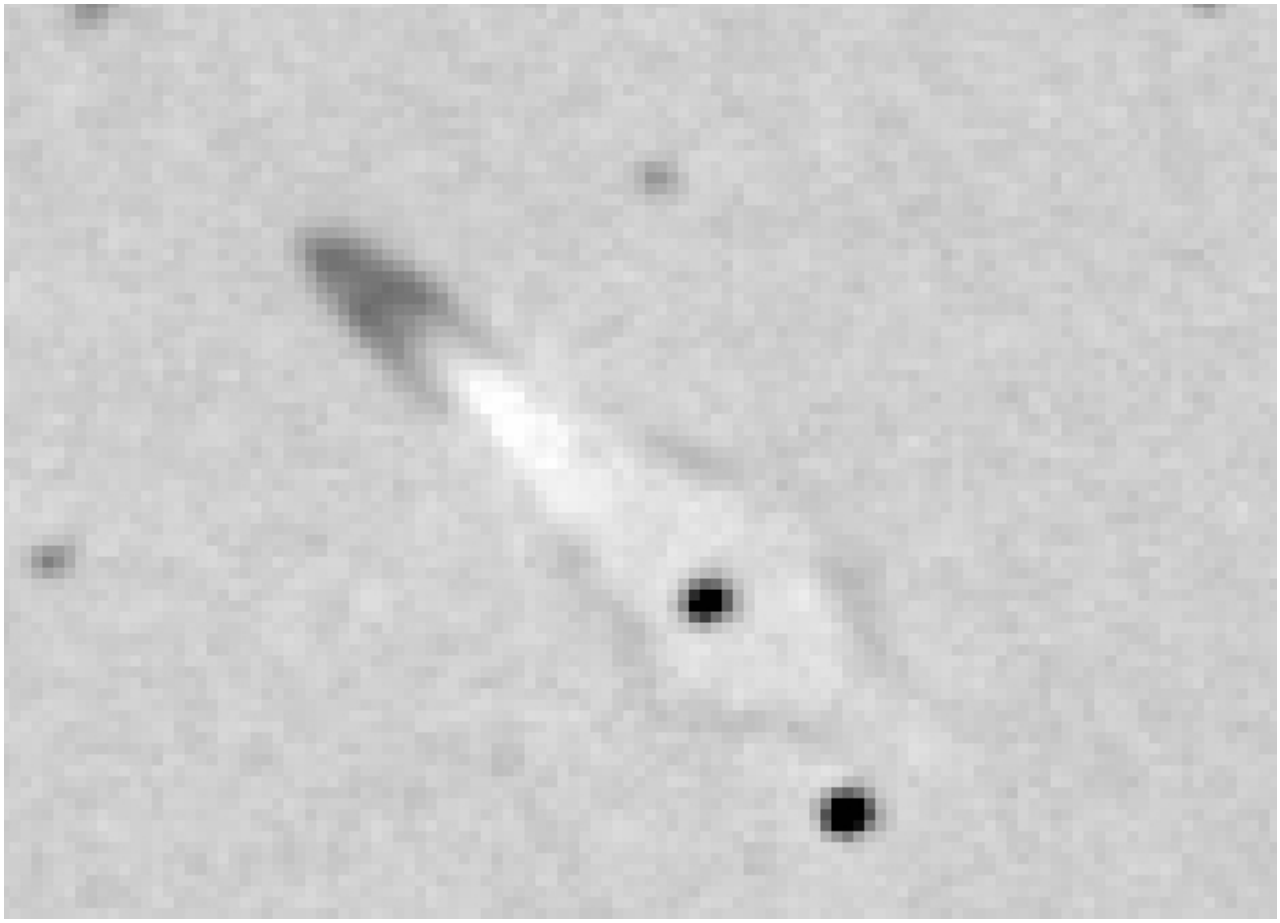

Fig. 6. Difference image between DCT and Palomar images showing changes in the Guitar Nebula head over the 19.3yr between observations. The pulsar has travelled at 0.18"/yr, and the surface brightness has dimmed in the interior, especially immediately behind the tip. Asymmetric expansion has also occurred perpendicular to the pulsar's proper motion. The sense of north is up, while east is left. The colormap is inverted.

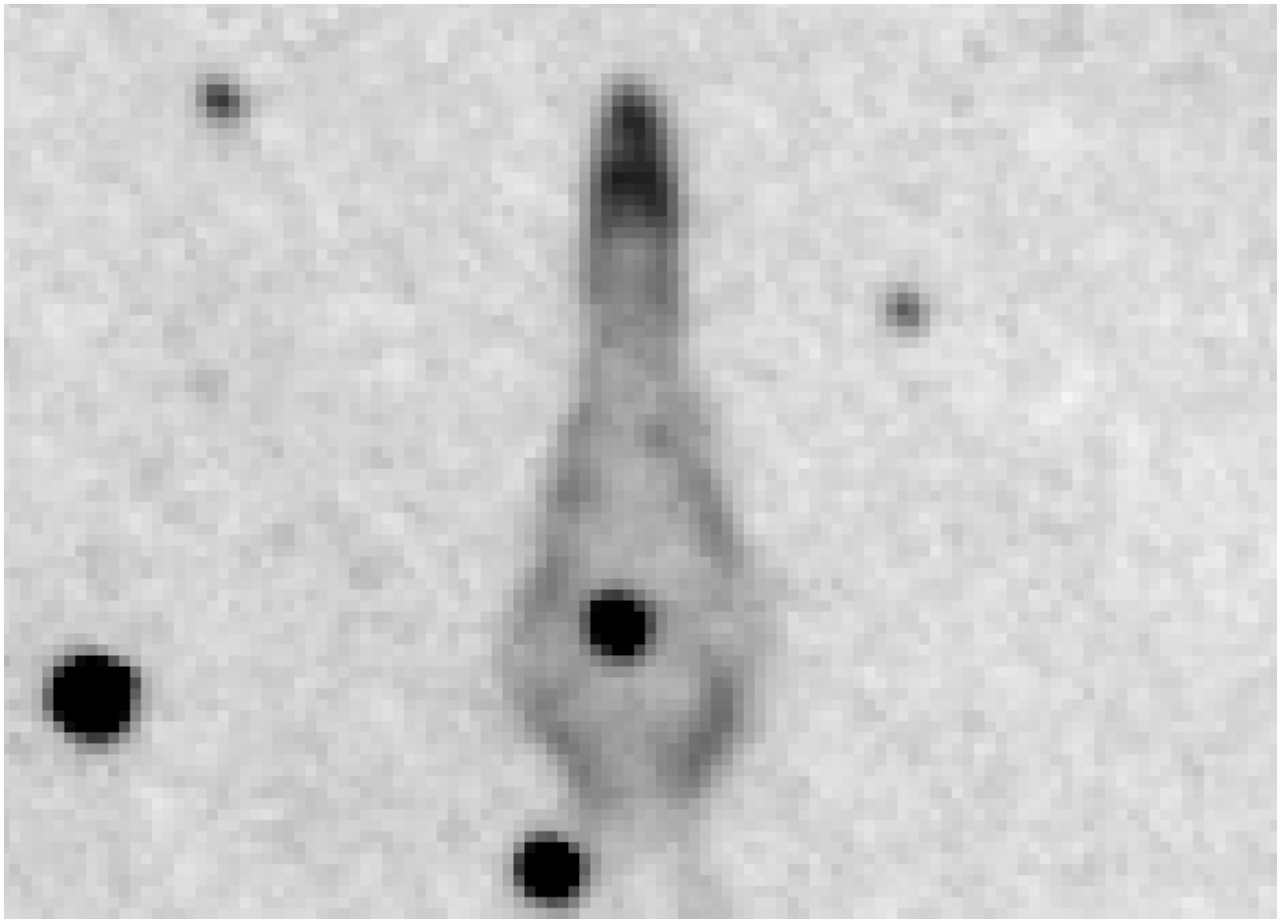

Fig. 7. DCT Hα ON image of the Guitar Nebula head, rotated by the nebula's effective position angle of 49.25°. In this view, the asymmetric, parallelogram-like structure of the limb-brightened edges becomes more apparent.

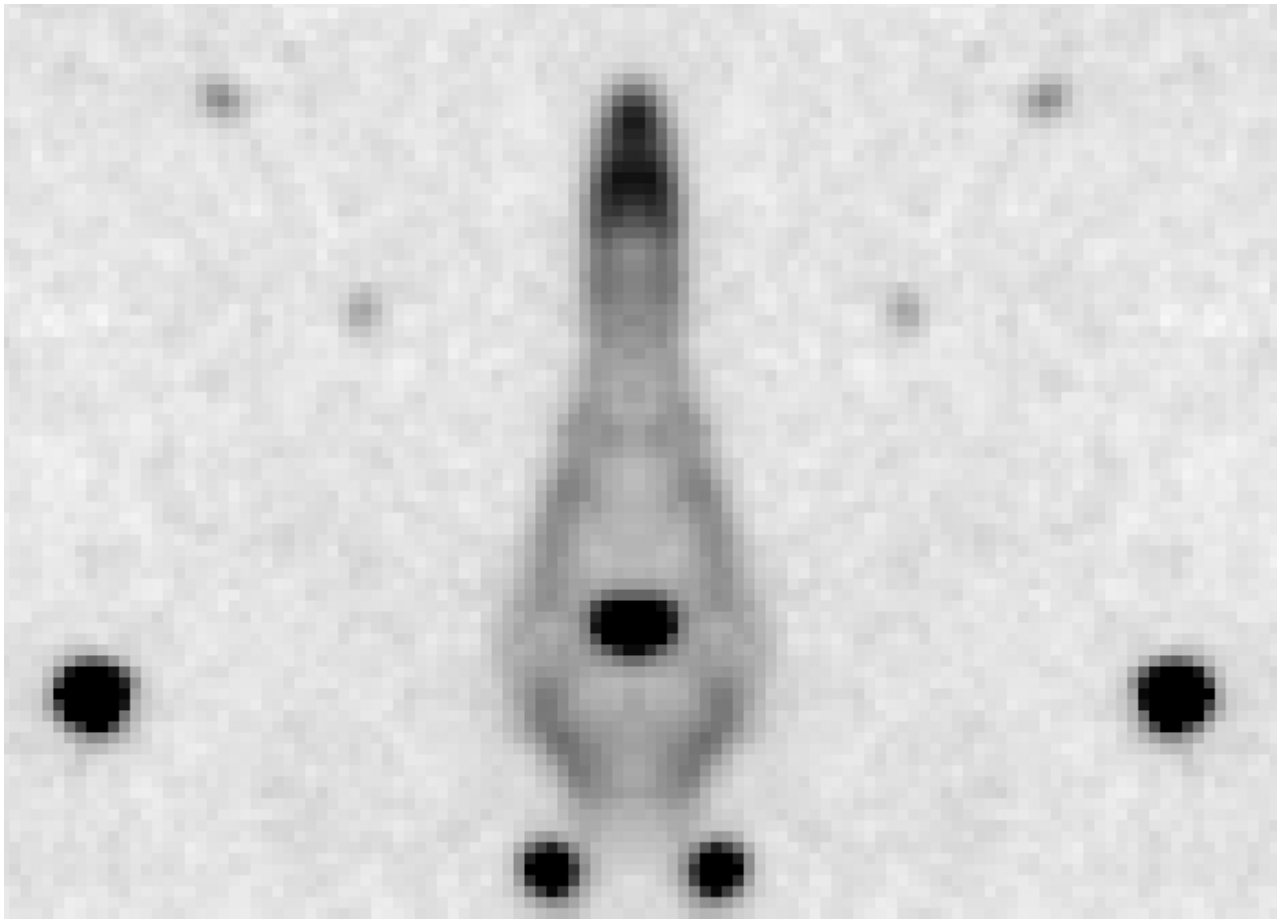

Fig. 8. Symmetric image of DCT Hα ON observation of the Guitar Nebula head, formed by mirroring the image along the symmetry axis and adding the images. The symmetric sub-structure at the tip becomes more pronounced.

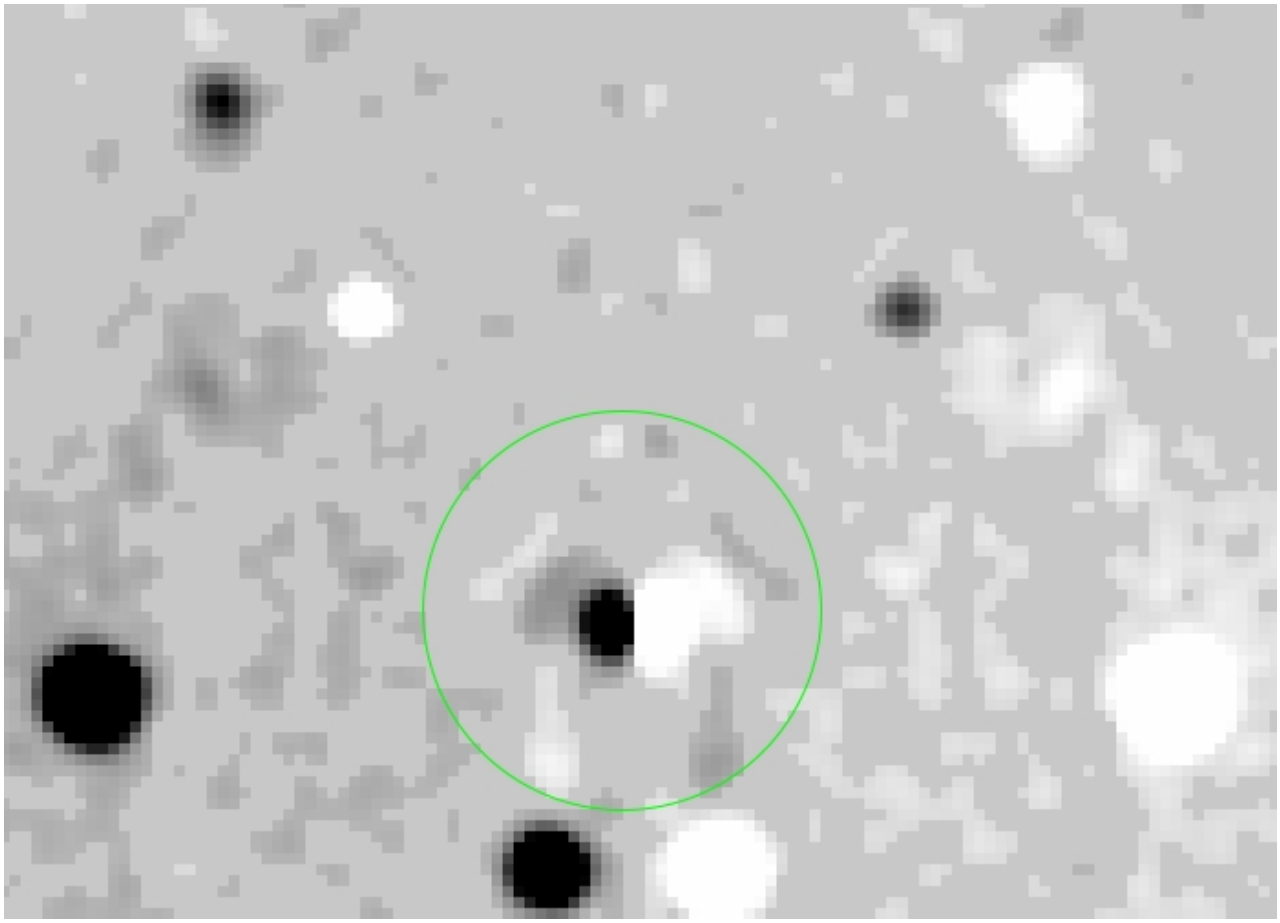

Fig. 9. Asymmetric image of the DCT Hα ON observation of the Guitar Nebula head. The each side is mirrored to the other, and the left – right difference images are computed and displayed. The resulting image is convolved with a Gaussian and noise is masked in order to emphasize the truly symmetric structures (see text for details). Asymmetries both in surface brightness and in spatial structure are apparent in the circled region, consistent with a density gradient in direction a different than the pulsar's proper motion.